

# Pre-submission seminar

## A study on the energy transfer of a body under fluid-elastic galloping

Supervisors:

Dr. Tan Boon Thong

Dr. Justin Leontini

Dr Huang Yew Mun



MONASH University  
Malaysia

# Flow induced vibrations can lead to structural failure



Source :[http://en.wikipedia.org/wiki/Tacoma\\_Narrows\\_Bridge\\_\(1940\)#mediaviewer/File:Image-Tacoma\\_Narrows\\_Bridge1.gif](http://en.wikipedia.org/wiki/Tacoma_Narrows_Bridge_(1940)#mediaviewer/File:Image-Tacoma_Narrows_Bridge1.gif)

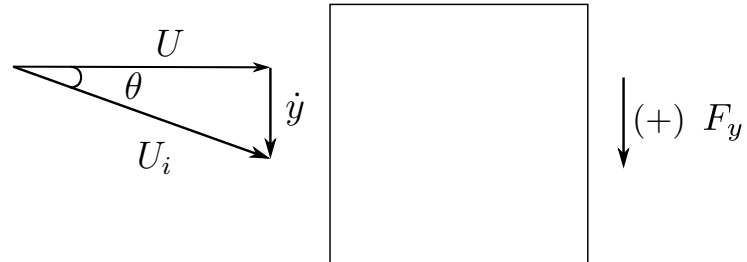


Source: <http://www.inmr.com/wp-content/uploads/2013/11/cover.jpg>

# This project consist of 3 phases

- Phase 1: Understand the underpinning parameters and formulate the appropriate variables of the system.
- Phase 2: Study the frequency response of the system, and the relationship with the formulated variables.
- Phase 3: Optimisation of the energy transfer by controlling the fluid mechanics of the system.

# Mechanism of galloping and Quasi-steady state hypothesis



$U$  Freestream velocity

$U_i$  Induced velocity

$U_i$  Induced velocity

$\theta$  Induced angle

$\dot{y}$  Transverse velocity

$C_L$  Coefficient of lift

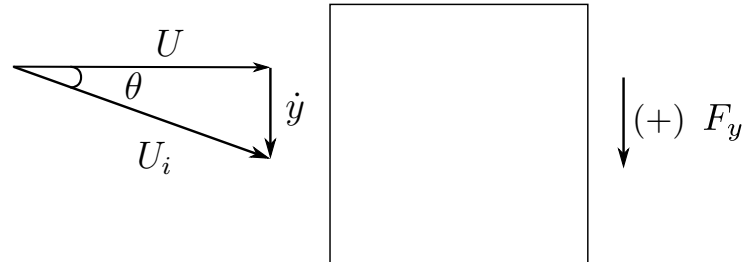
$C_d$  Coefficient of drag

$C_y$  Coefficient of transverse force

$F_y$  Transverse force



# Mechanism of galloping and Quasi-steady state hypothesis



$U$  Freestream velocity

$U_i$  Induced velocity

$U_i$  Induced velocity

$\theta$  Induced angle

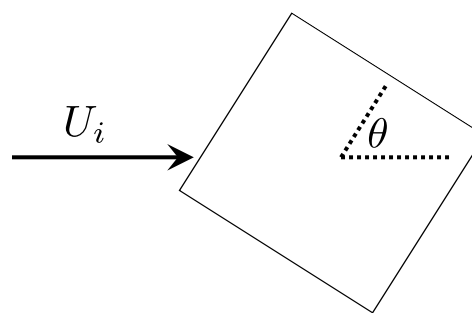
$\dot{y}$  Transverse velocity

$C_L$  Coefficient of lift

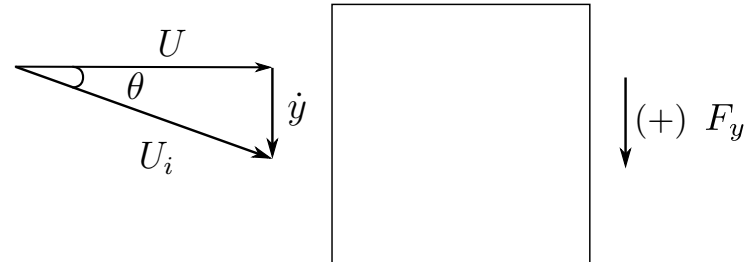
$C_d$  Coefficient of drag

$C_y$  Coefficient of transverse force

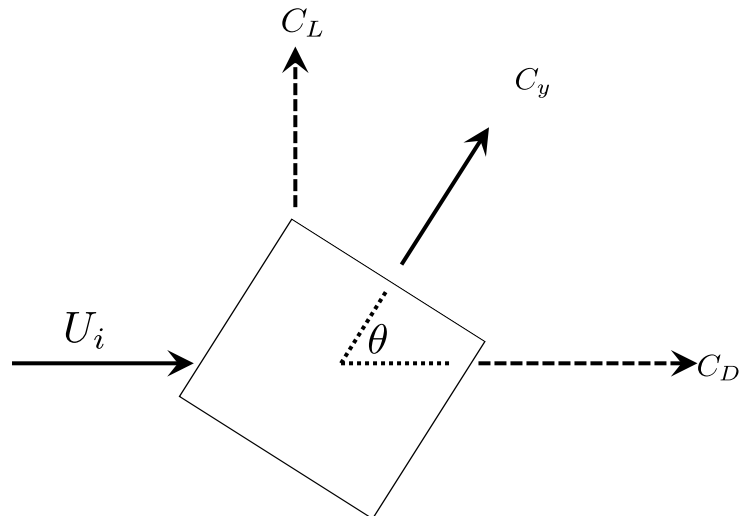
$F_y$  Transverse force



# Mechanism of galloping and Quasi-steady state hypothesis



$U$	Freestream velocity
$U_i$	Induced velocity
$U_i$	Induced velocity
$\theta$	Induced angle
$\dot{y}$	Transverse velocity
$C_L$	Coefficient of lift
$C_d$	Coefficient of drag
$C_y$	Coefficient of transverse force
$F_y$	Transverse force



## QSS model and mean power equations

$$m\ddot{y} + c\dot{y} + ky = \frac{1}{2}\rho U^2 \mathcal{A} \left( a_1 \left( \frac{\dot{y}}{U} \right) + a_3 \left( \frac{\dot{y}}{U} \right)^3 + a_5 \left( \frac{\dot{y}}{U} \right)^5 + a_7 \left( \frac{\dot{y}}{U} \right)^7 \right)$$

$$P_m = \frac{1}{T} \int_0^T (c\dot{y})\dot{y} dt$$

$$P_m = \frac{1}{T} \int_0^T F_y \dot{y} dt$$

# QSS model and mean power equations

$$m\ddot{y} + c\dot{y} + ky = \frac{1}{2}\rho U^2 A \left( a_1 \left( \frac{\dot{y}}{U} \right) + a_3 \left( \frac{\dot{y}}{U} \right)^3 + a_5 \left( \frac{\dot{y}}{U} \right)^5 + a_7 \left( \frac{\dot{y}}{U} \right)^7 \right)$$

$a_1, a_3, a_5, a_7$	Coefficients of the polynomial to determine $C_y$
$A = DL$	Frontal area of the body
$c$	Damping constant
$k$	Spring constant
$m$	Mass of the body
$U$	Freestream velocity
$\rho$	Fluid density
$y, \dot{y}, \ddot{y}$	Transverse displacement, velocity and acceleration of the body

## QSS model and mean power equations

$$m\ddot{y} + c\dot{y} + ky = \frac{1}{2}\rho U^2 \mathcal{A} \left( a_1 \left( \frac{\dot{y}}{U} \right) + a_3 \left( \frac{\dot{y}}{U} \right)^3 + a_5 \left( \frac{\dot{y}}{U} \right)^5 + a_7 \left( \frac{\dot{y}}{U} \right)^7 \right)$$

$$P_m = \frac{1}{T} \int_0^T (c\dot{y})\dot{y} dt$$

$$P_m = \frac{1}{T} \int_0^T F_y \dot{y} dt$$

$P_m$  Mean power

$F_y$  Instantaneous force normal to the flow

$t$  time

# Linearised QSS equation, natural time scales and non-dimensionalised parameters

$$m\ddot{y} + c\dot{y} + ky = \frac{1}{2}\rho U^2 \mathcal{A}a_1 \left( \frac{\dot{y}}{U} \right)$$

$$\lambda_{1,2} = -\frac{1}{2} \frac{c - \frac{1}{2}\rho U \mathcal{A}a_1}{m} \pm \frac{1}{2} \sqrt{\left[ \frac{c - \frac{1}{2}\rho U \mathcal{A}a_1}{(m)} \right]^2 - 4\frac{k}{m}}.$$

$$\Pi_1 = 4\pi^2 m^{*2}/U^{*2}$$

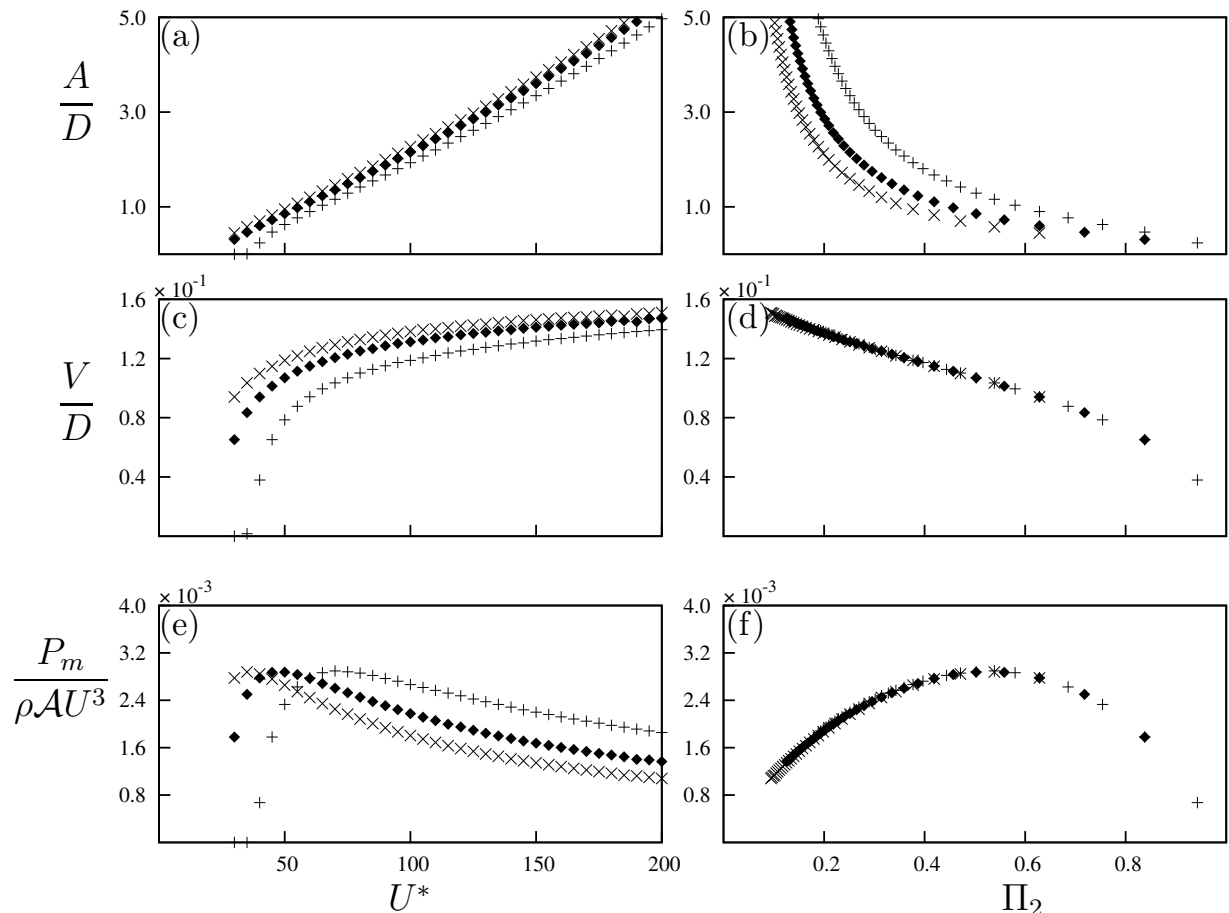
$$\Pi_2 = c^* m^*$$

$\lambda_{1,2}$	Eigenvalues of linearised equation of motion
$m^* = m/\rho D^2 L$	Mass ratio
$U^* = U/fD$	Reduced velocity
$c^* = cD/mU$	Non-dimensionalised damping factor
$\Pi_1 = 4\pi^2 m^{*2}/U^{*2}$	Combined mass-stiffness parameter
$\Pi_2 = c^* m^*$	Combined mass-damping parameter

# Classical VIV parameters vs. New Parameters

$$Re = 200 \\ m^* = 20$$

- $\zeta = 0.075$  ( $\times$ )
- $\zeta = 0.1$  ( $\blacklozenge$ )
- $\zeta = 0.15$  ( $+$ )



$A$  Displacement amplitude  
 $V$  Velocity amplitude

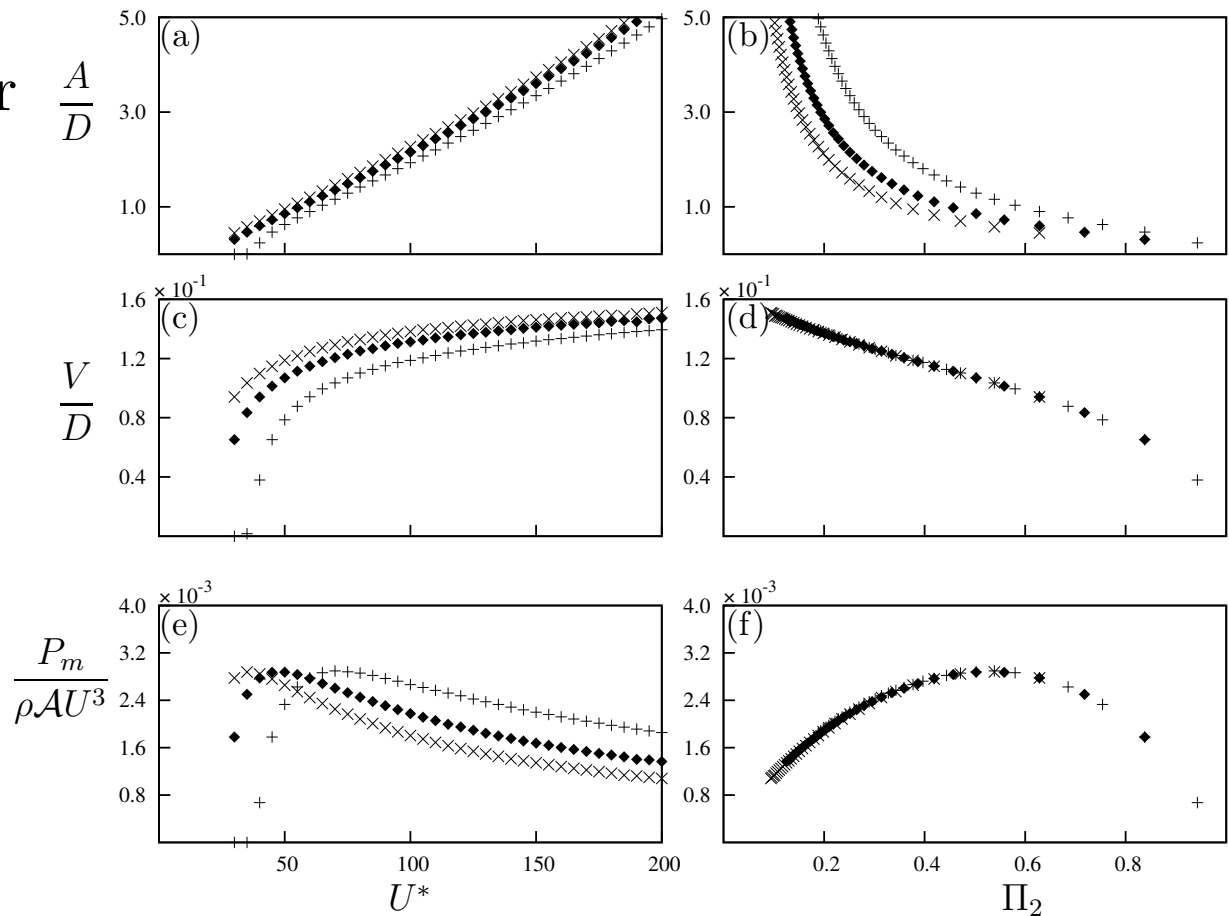
# Classical VIV parameters vs. New Parameters

$\Pi_2$  provides a better collapse of the data

$$Re = 200$$

$$m^* = 20$$

- $\zeta = 0.075$  ( $\times$ )
- $\zeta = 0.1$  ( $\blacklozenge$ )
- $\zeta = 0.15$  ( $+$ )



$A$  Displacement amplitude  
 $V$  Velocity amplitude

A good agreement between QSS and DNS results could be obtained at high  $\Pi_1$

$Re = 200$

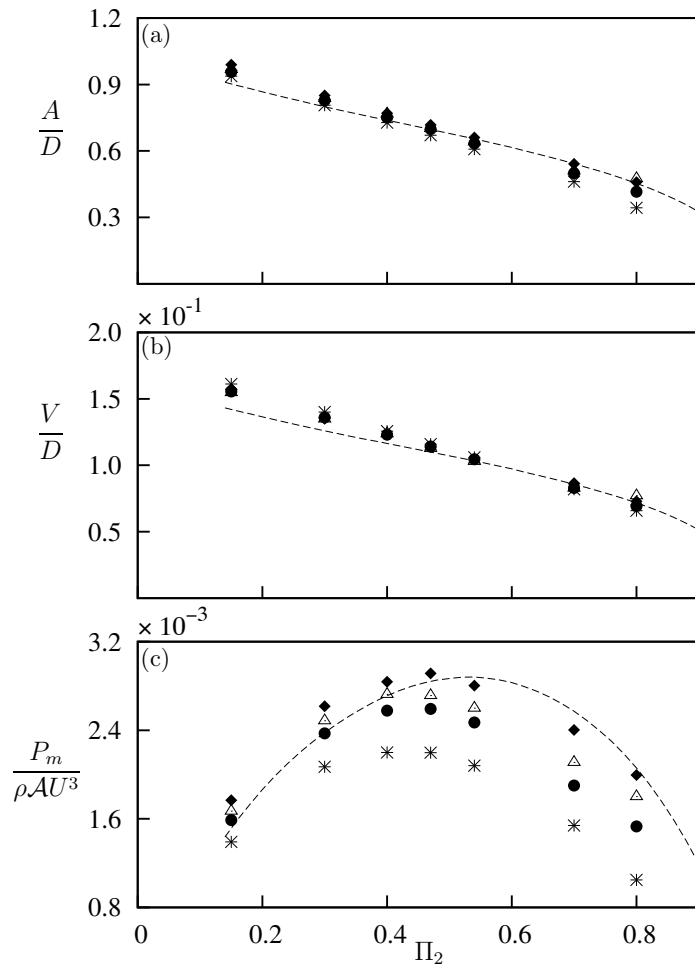
$\Pi_1 = 10$  ( $m^* = 20.13$ ) (\*)

$\Pi_1 = 60$  ( $m^* = 49.31$ ) (●)

$\Pi_1 = 250$  ( $m^* = 100.7$ ) ( $\triangle$ )

$\Pi_1 = 1000$  ( $m^* = 201.3$ ) (◆)

QSS data at  $\Pi_1 = 10$  (---)



Clear wavelength is visible in the flow as  $\Pi_1$  is increased

Vorticity plots at arbitrary instants at  $\Pi_2 = 0.47$ .

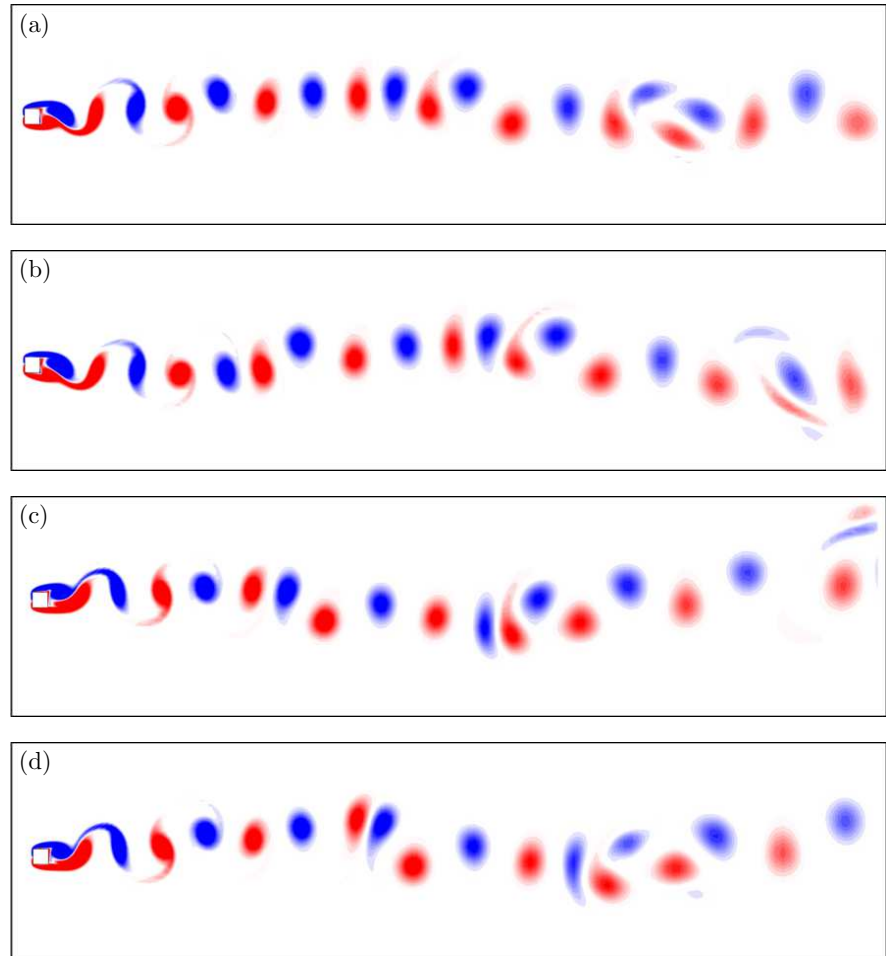
(a)  $\Pi_1 = 10$

(b)  $\Pi_1 = 60$

(a)  $\Pi_1 = 250$

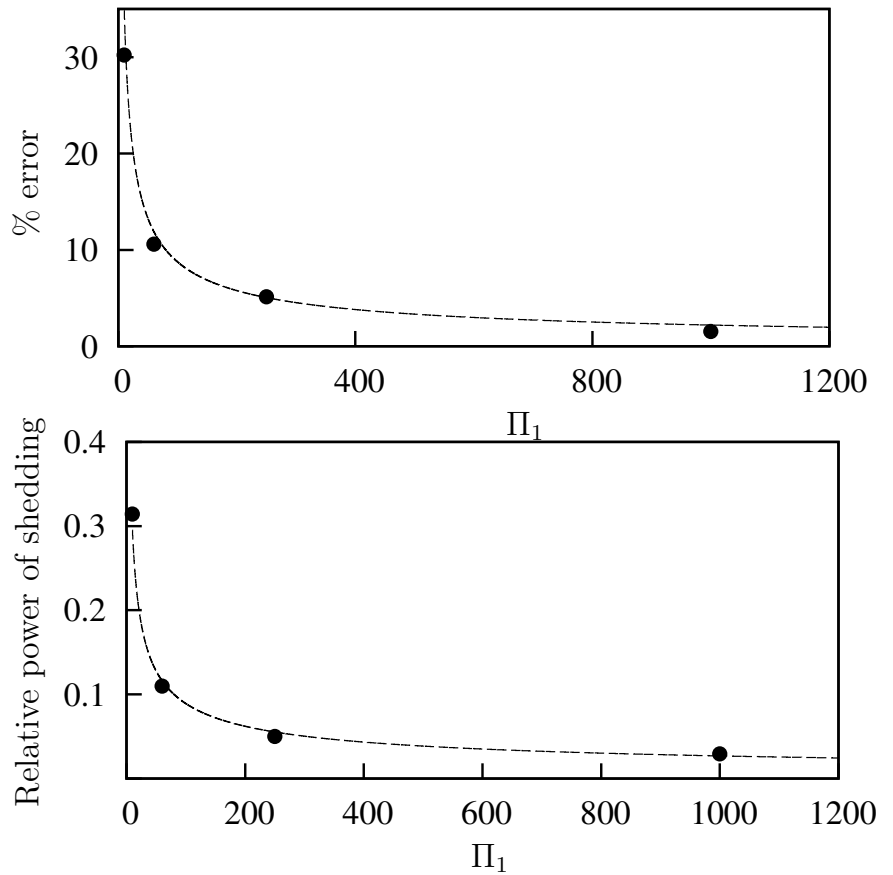
(d)  $\Pi_1 = 1000$

$f_{input} = 0.025$



Relative power of shedding and % error of power between QSS and DNS is an inverse function of  $\Pi_1$

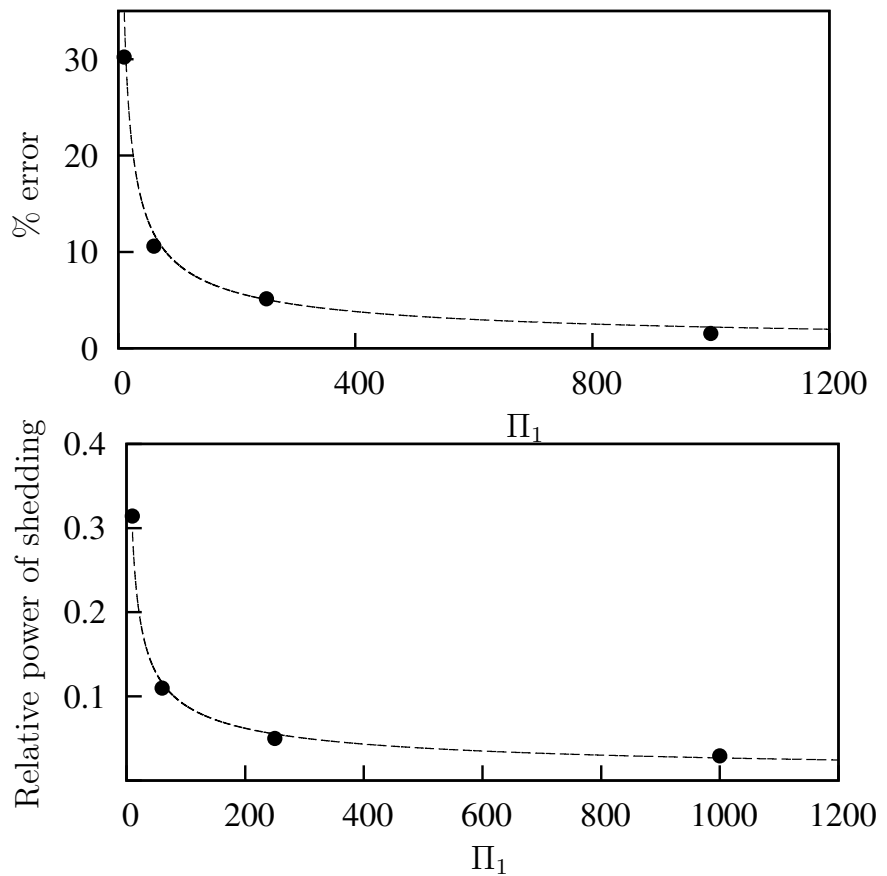
$$\% \text{ error} = \left| \frac{P_{m(QSS)} - P_{m(DNS)}}{P_{m(DNS)}} \right| \times 100.$$



Relative power of shedding and % error of power between QSS and DNS is an inverse function of  $\Pi_1$

$$\% \text{ error} = \left| \frac{P_{m(QSS)} - P_{m(DNS)}}{P_{m(DNS)}} \right| \times 100.$$

$$\% \text{error} = 138.697 \Pi_1^{-0.6}$$

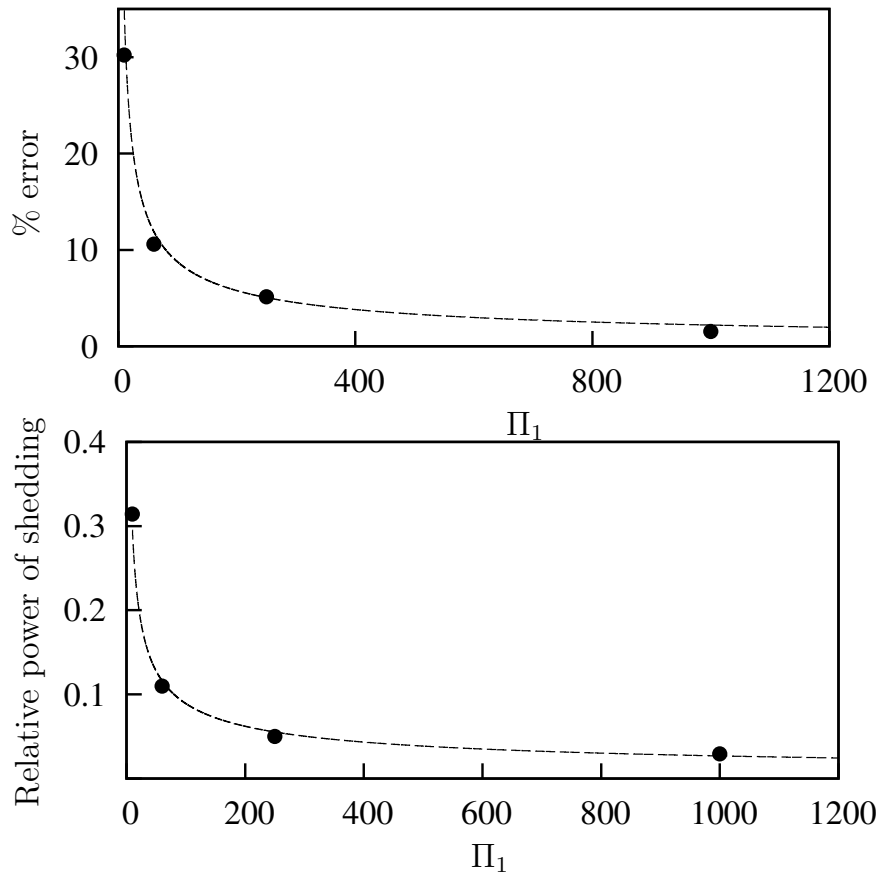


Relative power of shedding and % error of power between QSS and DNS is an inverse function of  $\Pi_1$

$$\% \text{ error} = \left| \frac{P_{m(QSS)} - P_{m(DNS)}}{P_{m(DNS)}} \right| \times 100.$$

$$\% \text{error} = 138.697 \Pi_1^{-0.6}$$

$$\text{Relative power} = 0.977 \Pi_1^{-0.52}$$



# Conclusions from phase 1

- $\Pi_1$  and  $\Pi_2$  provide a good collapse compared to the classical VIV parameters,  $U^*$  and  $\zeta$ .
- The velocity amplitude and the power transfer does not depend on the natural frequency of the system over a large range of frequencies.
- Quasi-steady state model provides a good prediction of power output in comparison with DNS data of the system when  $\Pi_1$  is relatively high.
- As  $\Pi_1$  is decreased, the deviation between QSS and DNS data increases as the influence of vortex shedding becomes more stronger.

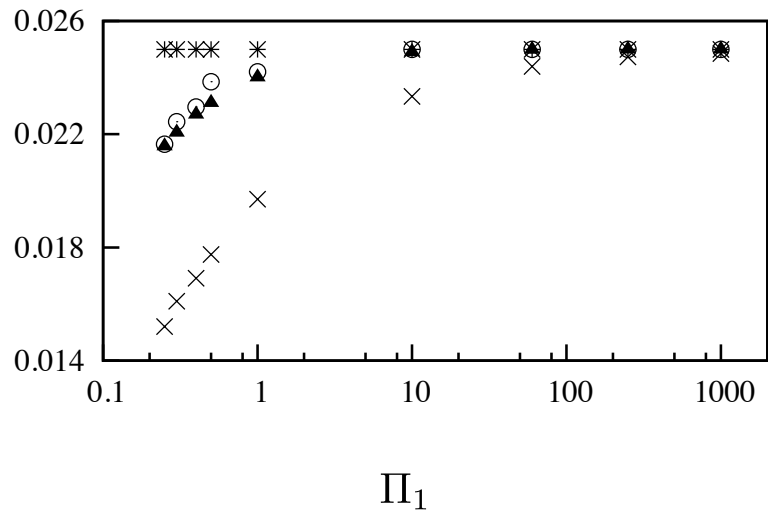
# Effect of $\Pi_1$ and non-linear effects on galloping frequency

$$\frac{\lambda D}{U} = \frac{1}{2} \left( \Pi_2 - \frac{1}{2} \right) \pm \sqrt{\Pi_2^2 - \Pi_2 a_1 + \frac{a_1^2}{4} - 4\Pi_1}$$

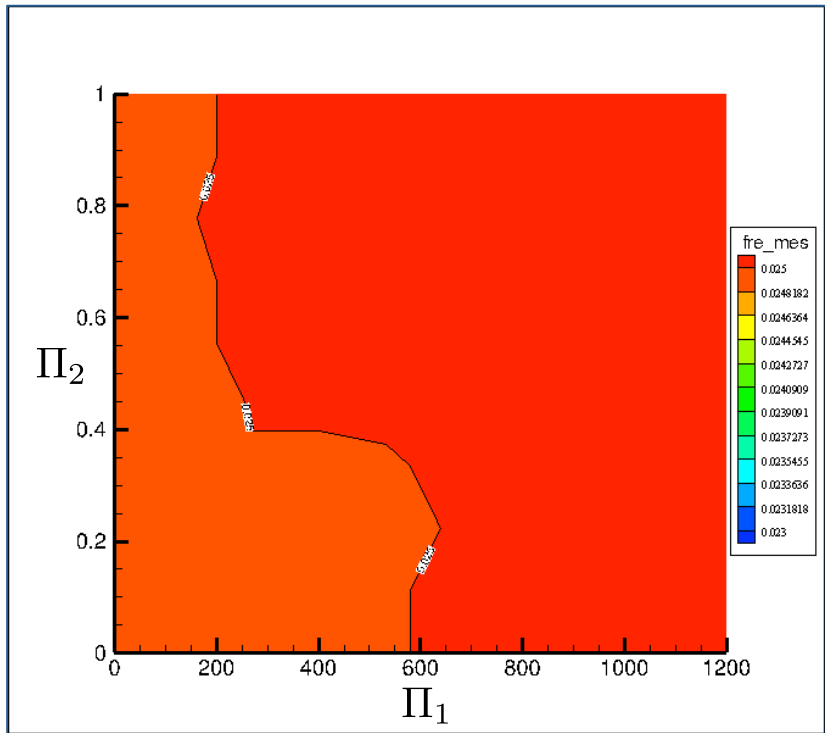
$$f_{input} = 0.025$$

- $f_{input}$  (\*)
- $f_{linear}$  (○)
- $f_{QSS}$  (▲)
- $f_{DNS}$  (×)

$$\frac{fD}{U}$$

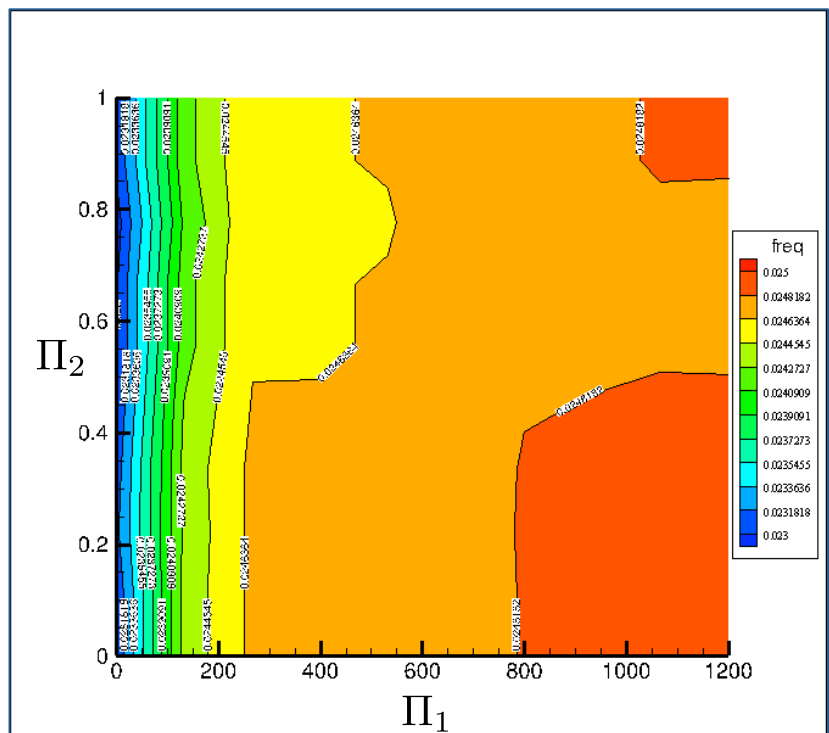


# Frequency data in $\Pi_1$ and $\Pi_2$ space



QSS frequency data (freq\_mes)

$$f_{input} = 0.025$$



DNS frequency data (freq)

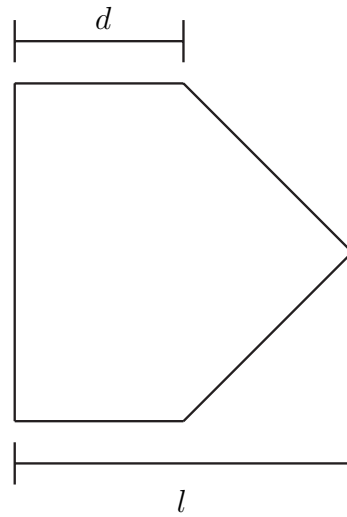


# Conclusions from phase 2

- The linear frequency of the system could be obtained from the imaginary component of the eigenvalue equation of the linearised QSS model.
- This equation provides a good prediction of the frequency at high  $\Pi_1$ . However, it deviates as  $\Pi_1$  reduces due to non linear forcing.
- The linearised equation fails to predict the frequency at the point where the term under the square root positive. However, the general QSS model does output a frequency.
- The region where the linear expression of frequency fail could not be captured in the DNS data, as the vortex shedding becomes stronger and therefore suppresses galloping.

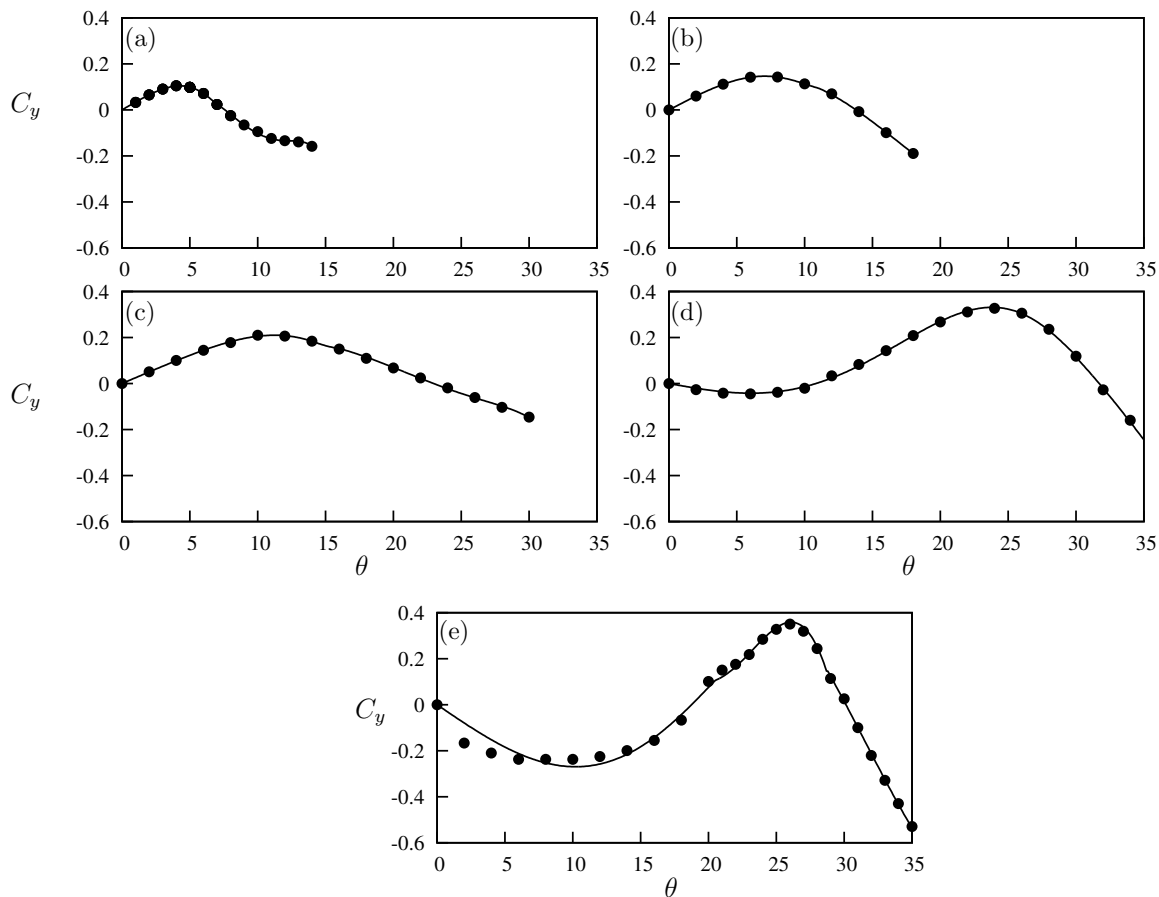


# Delaying the shear layer re-attachment



# Delaying the shear layer re-attachment

- (a) square
- (b)  $\frac{d}{l} = 0.75$
- (c)  $\frac{d}{l} = 0.5$
- (d)  $\frac{d}{l} = 0.25$
- (e) triangle.

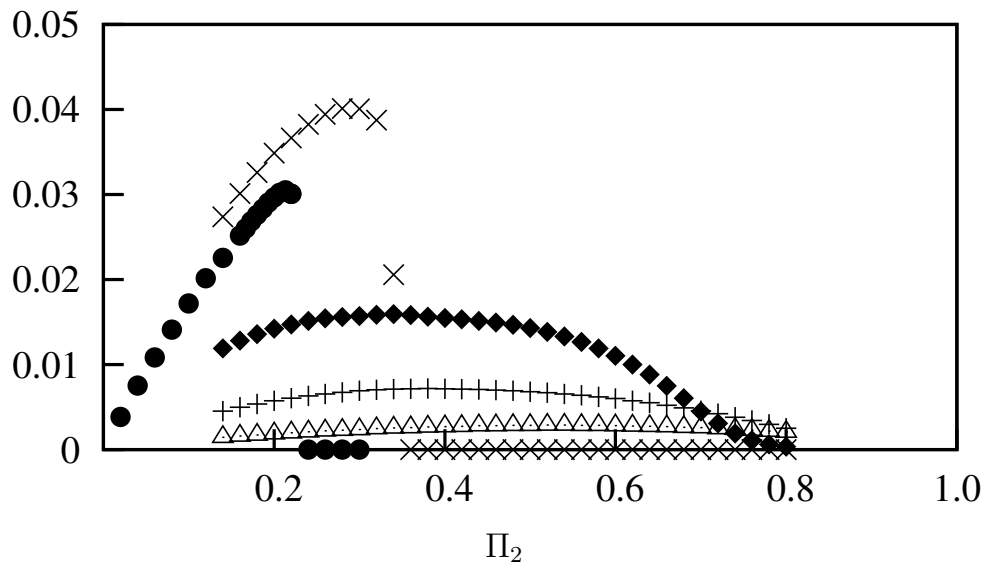


# Dimensionless mean vs. $\Pi_2$ for five selected cross sections

$\frac{P_m}{\rho \mathcal{A} U^3}$

- square  $(\triangle)$
- $\frac{d}{l} = 0.75$   $(+)$
- $\frac{d}{l} = 0.5$   $(\blacklozenge)$
- $\frac{d}{l} = 0.25$   $(\times)$
- triangle  $(\bullet)$

QSS data at  $Re = 200$ ,  $\Pi_1 = 100$



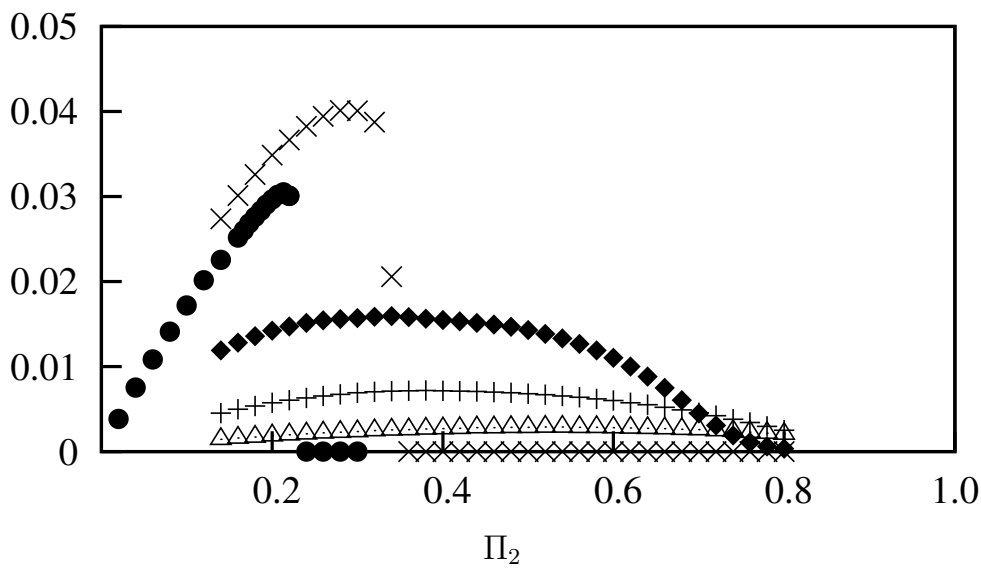
# Dimensionless mean vs. $\Pi_2$ for five selected cross sections

The optimal ratio lies around

$$\frac{d}{l} = 0.25$$

- square  $(\triangle)$
- $\frac{d}{l} = 0.75$   $(+)$
- $\frac{d}{l} = 0.5$   $(\blacklozenge)$
- $\frac{d}{l} = 0.25$   $(\times)$
- triangle  $(\bullet)$

$$\frac{P_m}{\rho \mathcal{A} U^3}$$



QSS data at  $Re = 200$ ,  $\Pi_1 = 100$

# Preliminary conclusions from phase 3

- Delaying the shear layer reattachment could lead to a higher power output. This was carried out by tapering away of the top and bottom surfaces of the square.
- As  $\frac{d}{l}$  was reduced, a negative segment of the lift curve emerged which in return resulted in power transfer from the body to the fluid.
- Within the  $\frac{d}{l}$  ratios tested, the optimal ratio lies around  $\frac{d}{l} = 0.25$  .

# Publications

- Jayatunga, H.G.K.G., Tan B.T., Leontini J.S., A study on the energy transfer of a square prism under fluidelastic galloping. *Journal of Fluids and Structures* (2015),  
<http://dx.doi.org/10.1016/j.jfluidstructs.2015.03.012>
- Leontini J.S., Zaho J., Jayatunga H.G.K.G., Lo Jacono D., Tan B.T., Sheridan J., 2014 'Frequency Selection and Phase Locking during Aeroelastic Galloping' presented to the 19th Australasian Fluid Mechanics Conference Melbourne, Australia 8-11 December 2014